

Paweł ZAWADZKI*, **Natalia WIERZBICKA****, **Rafał TALAR*****, **Łukasz BURYSZ******

TRIBOLOGICAL PROPERTIES OF HARDENED SURFACES CONSTITUTED BY VARIOUS METHODS OF MECHANICAL PROCESSING

WŁAŚCIWOŚCI TRIBOLOGICZNE UTWARDZONYCH POWIERZCHNI UKONSTYTUOWANYCH RÓŻNYMI METODAMI OBRÓBKI MECHANICZNEJ

Key words:

dry friction, wear, friction coefficient, machining methods.

Abstract:

The paper presents the results of experimental studies involving the determination of the coefficient of friction (COF) of surfaces constituted by selected machining methods. The tests were carried out on a Bruker UMT2 stand using a ball made of 100Cr6 steel with a hardness of 62 HRC and a disc made of X210CR12 (NC11LV) steel with a hardness of 62 ±0.4 HRC in dry conditions. During the research, wear products were not removed from the sliding path. The paper presents methods of producing samples and corresponding surface characteristics. Significant differences in topography characterised the surfaces obtained due to various machining. The COF values at the beginning of the study and the COF values occurring after a specific route in the reciprocating cycle reached similar values, despite the significant differences in the surface topography of the tested samples. Significant COF changes as a path function were observed for samples produced with different machining methods.

Słowa kluczowe:

tarcie suche, zużycie, współczynnik tarcia, metody obróbki.

Streszczenie:

Praca przedstawia wyniki badań doświadczalnych obejmujących wyznaczenie współczynnika tarcia (COF) powierzchni ukonstytuowanych wybranymi metodami obróbki mechanicznej. Badania przeprowadzono na stanowisku Bruker UMT2 bez stosowania medium smarującego w skojarzeniu kulki stalowej wykonanej ze stali 100Cr6 (ŁH15) o twardości 62 HRC i dysku stalowego wykonanego ze stali X210CR12 (NC11LV) o twardości 62 ±0.4 HRC. W trakcie prowadzenia badań produkty zużycia nie były usuwane ze strefy ruchu. W pracy przedstawiono sposoby wytworzenia próbek i odpowiednio charakterystyki powierzchni. Otrzymane w wyniku różnych sposobów obróbki powierzchnie charakteryzowały się dużymi różnicami ich topografii. Wartości COF występujące na początku badania i wartości COF występujące po przebyciu określonej drogi w cyklu posuwisto-zwrotnym osiągały zbliżone wartości pomimo znacznych odrębności topografii powierzchni badanych próbek. Zaobserwowano istotne różnice przebiegu zmian COF w funkcji drogi dla próbek wytworzonych odmiennymi metodami obróbki mechanicznej.

* ORCID: 0000-0001-8153-8774. Poznan University of Technology, Faculty of Mechanical Technology, M. Skłodowska-Curie Square 5, 60-965 Poznań, Poland, e-mail: pawel.zawadzki@put.poznan.pl.

** ORCID: 0000-0002-4862-6534. Poznan University of Technology, Faculty of Mechanical Technology, M. Skłodowska-Curie Square 5, 60-965 Poznań, Poland.

*** ORCID:0000-0003-4355-9923. Poznan University of Technology, Faculty of Mechanical Technology, M. Skłodowska-Curie Square 5, 60-965 Poznań, Poland.

**** ORCID:0000-0003-4355-9923. Poznan University of Technology, Faculty of Mechanical Technology, M. Skłodowska-Curie Square 5, 60-965 Poznań, Poland.

INTRODUCTION

Friction is the totality of physical phenomena accompanying the movement of two physical bodies against each other, touching each other (external friction) or elements of the same body (internal friction) and causing energy to dissipate during movement. External friction occurs at the border of two solids, while internal friction occurs during the flow of fluids and deformation of solids. It is significant in many fields of science, because it can be intentional, deliberately induced, increased, or possibly reduced. There are many ways to reduce friction, but while selecting a method, the economic issues should be considered, i.e. whether it is necessary. This decision requires knowledge of the behaviour and wear mechanism of the contacting bodies. It allows determining in which situations the reduction of frictional forces is essential and in which it is not significant [L. 1]. Various traces can be obtained on the treated surface, depending on the finishing. This phenomenon is called the directionality of the geometric structure of the surface. The quality of the product's top layer finish significantly impact its operational and wear properties. Therefore, it is necessary to examine a given layer's geometric and physical properties to determine its performance quality. The surface quality determines the condition of unevenness and the state of the top layer [L. 2, 3]. The basic operations that positively affect the quality of the surface layer include heat and thermochemical treatment, electroplating, and all kinds of fine abrasive, chip, and plastic treatments [L. 3].

Nowadays, more and more emphasis is placed on the possible reduction of frictional resistance between machine parts, thus reducing the power required to move these bodies. To do this, particular attention should be paid to the factors influencing the friction between the surfaces. The results of many studies show that surfaces machined with different methods may have roughness levels of similar size and have significantly different friction coefficients, based on which, it can be concluded that the roughness parameter can be used to approximate the usefulness of a given surface. Still, it is impossible to define its more specific tribological properties [L. 4–6]. Sedlacek et al. in paper [L. 6] performed on surfaces machined by turning and milling, using different machining parameters for each sample, and it can be seen that the coefficient of friction (COF) was lower for the smoother surface, but this is visible only for pieces

machined with high rotational speed (which reduces the feed per revolution). It can be determined that the distance travelled during the test to obtain a stabilised coefficient of friction increased with increasing roughness [L. 7–9]. Additionally, the author proved that the distance travelled during the test to the normalised coefficient of friction increased with increasing roughness.

The main objective of the research was to determine the behaviour of the coefficient of friction on surfaces obtained by various processing methods, taking into account the directionality of the surface layer obtained after these treatments.

MATERIALS AND METHODS

Samples preparation

The paper presents the results of experimental tests involving the determination of the friction coefficient of surfaces constituted by selected machining methods. The samples were made of X153CrMo1V12 (NC11LV) steel and are characterised by good hardenability and abrasion resistance; additionally, it has been heat-treated (hardening at 1020°C and tempering at 200°C), resulting in a hardness of 62 ±0.4 HRC. The samples were made of a rod diameter of 72 mm and then prepared for wear tests. The semi-finished products prepared in this way were subjected to heat treatment, hardening, and tempering [L. 10]. A 3/8 inch diameter bearing ball made of 100Cr6 steel was used as a counter-sample. The mechanical properties of the materials are presented in **Table 1**.

Table 1. Basic mechanical properties of the sample and the counter sample

Tabela 1. Podstawowe właściwości mechaniczne próbki i przeciwpóbkki

Steel type	Elastic modulus GPa	Hardness HRC	Density g·m ⁻³
100Cr6	210[L. 11]	62 [L. 12]	7.85 [L. 12]
NC11LV	210 [L. 13]	62 ±0.4	7.6 [L. 13]

Raw samples of NC11LV steel in discs were subjected to grinding treatment using a surface grinder and a magnetic table. The task aimed to minimise the non-parallelism of the mounting plane in the tribotester holder and the test plane. In the next stage, one of the ground surfaces was subjected to a specific treatment, and then the samples were secured. The final process methods

and devices on which the planes were machined are as follows: Doosan Lynx 220LSY – rough turning, finishing turning, Doosan DVF 5000 – rough milling, finishing milling, spiral milling, Jotes SJW 1000 – coarse flat grinding, Jotes SPC 20 – flat finishing grinding, face grinding, VIRGO PK350EZ – sanding, and Erba EVP-RA – polishing.

Surface morphology and topography test

The properties of the surface layer of the samples were tested with an Alicona InfiniteFocus UR-10 optical profilometer. The tests were carried out

following ISO 25178, and the roughness, waviness, surface bearing capacity, structure directivity, and an approximate image of the surface with the dimensions of unevenness were measured. The tests were repeated ten times on the frontal surface.

Tribological tests

The tests were performed in the pin on plate variant using the BRUKER UMT-2 Tribolab laboratory tribotester following the PN-EN 1071-12 standard.

The test was carried out under a constant force of 10 N at a speed of 10 mm/s for 15 min.

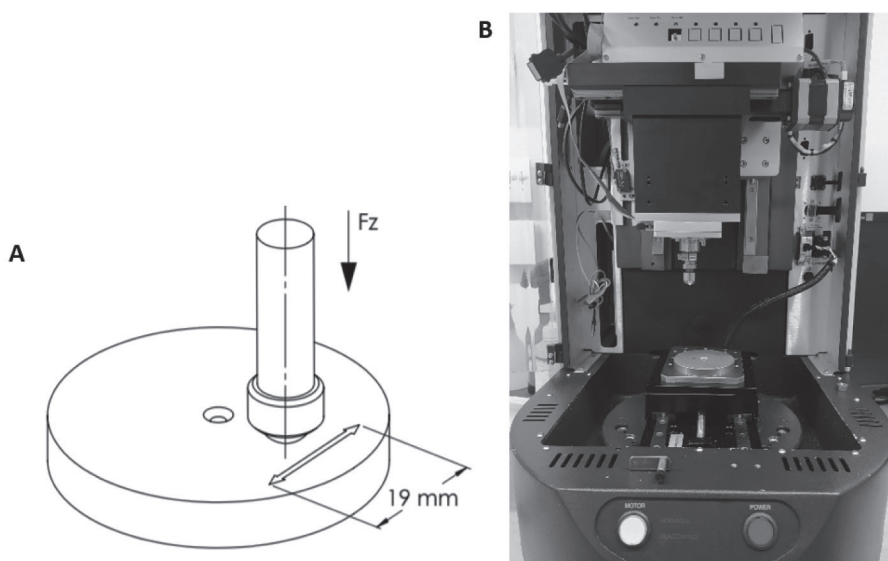


Fig. 1. The scheme of reciprocating motion (A) used during tribological tests, F_z – pressure force, range of motion was 19 mm and test stand – Bruker UMT (B)

Rys. 1. Schemat ruchu posuwisto-zwrotnego (A) zastosowany podczas badań tribologicznych, F_z – siła nacisku, zakres ruchu 19 mm oraz stanowisko badawcze – Bruker UMT (B)

Table 2. Basic parameters implemented during the tests: F_z – pressure force, p_{max} – maximum stresses in the contact zone, τ_{max} – maximum shear stresses in the contact zone, z – depth of maximum stresses, d – theoretical contact zone diameter, v – movement velocity, s – movement range and t – test time

Tabela 2. Podstawowe parametry zastosowane podczas badań: F_z – siła nacisku, p_{max} – maksymalne naprężenia w strefie kontaktu, τ_{max} – maksymalne naprężenia ścinające w strefie kontaktu, z – głębokość maksymalnych naprężeń, d – teoretyczna średnica strefy kontaktu, v – prędkość ruchu, s – zakres ruchu i czas testu t

Parameter	F_z	p_{max}	τ_{max}	z	d	v	s	t
Value	10 N	1034.6 MPa	325.5 MPa	32 μm	136 μm	10 mm/s	19 mm	15 min

The measuring section was 19 mm. The test object was screwed to the machine table to prevent its movement during the test. A 3/8 inch bearing ball, made of 100Cr6 steel, was mounted longitudinally to a Z-axis. The sample's surface and the balls have been cleaned using methanol to remove contamination. The tests were performed in

a laboratory with a constant temperature of 20°C and 50% humidity.

During the test, the bearing ball was in constant contact with the sample surface, making a reciprocating motion along the X-axis of the machine. For all samples, measurements were carried out in two directions: perpendicular and

parallel to machining traces. In all cases, the paths were perpendicular to each other. After each test (one track), the ball was replaced with a new one. The machine's software measured and recorded the current position, friction coefficient, and the force applied to the sample surface throughout the test.

Additionally, the potential influence of the roughness peaks as well as the presence of oxides on the sample surface on the friction coefficient was measured. For this purpose, the measurements were performed in two variants: the movement of the pin on the target and the spiral movement. The sample rotated and the location made a sliding movement towards the centre of the element. This movement allowed the counter-sample to move continuously over the intact surface of the sample. The test results were compared with other effects in order to confirm the hypothesis that moving on an intact surface with a higher Sq parameter results in a lower friction coefficient, and that the presence of oxides on the sample surface may stabilize coefficient of friction through their accumulation in the contact space of the elements.

Microscopy analysis

Detailed observations were made using a Tescan Vega 5135 scanning electron microscope to analyse the specific deformation of the dynamically charged surface of the samples. The surfaces of the pieces after the friction wear resistance test process were also subjected to EDS (Energy Dispersive Spectroscopy) analysis to examine the generated tribofilm on the surface of the cooperating materials.

RESULTS AND DISCUSSION

Before starting the research, the theory was adopted that the initial and final coefficient of friction on all samples should be almost identical. It was supposed to result from a layer of adsorbed oxides [L. 14] on the surface, which lubricant. These assumptions were confronted with the EDS analyses and SEM photos included in the other part of the chapter. The final stage was to normalise the friction coefficient on the graph due to rubbing the ball or sample and smoothing the surface. The device emitted a characteristic squeaky noise caused by the dry friction of hard surfaces rubbing against each other. The sound slightly changed depending on the surface of the currently tested sample. The tests were performed in two different positions and

directions, and it was to notice possible differences in the coefficient due to the other arrangement of the surfaces.

Surface morphology and topography

Among the results of surface topography measurements, the most important in terms of the research carried out was the following: the mean square deviation of the surface unevenness height from the reference plane Sq , maximum surface peak height Sp , maximum surface recess height Sv , maximum surface height Sz , and the arithmetic mean height of the surface Sa . This parameter allows defining the surface's complexity range and thus the size of the possible contact surface (see **Tab. 3**).

Table 3 shows all the relevant surface roughness parameters after specific treatments. Among the indicated data, the most critical surface development may be the mean square deviation of the surface unevenness height from the reference plane Sq and the arithmetic mean height of the surface Sa . The larger the values of Sa and Sq are, the length of the contact path against the sample with the surface decreases, which results in changes in the distribution of contact stresses. Due to the precise directivity of the surface topography (excluding the sample after sandblasting), tribological measurements were carried out in two directions. These directions are marked with black arrows in the roughness diagrams in **Tab. 3**.

The results of Sa and Sq measurements are shown in **Fig. 2**. The highest Sq values characterise the surface after grinding, rough milling, and coarse flat grinding. Another group consists of surfaces after finishing turning, surface grinding, rough turning, rough milling, and finishing milling. The most negligible surface development in Sq is characterised by finishing polishing, coarse polishing, and finishing flat grinding. The highest Sa values characterise rough turning, finishing turning, and face grinding. In other cases, similar values were obtained. The obtained results were used to find a correlation with the process of sample surface wear. **Figures 3a** and **3b** show the digitised surface topography after applying a Gaussian filter. A clear difference is noticeable in the combination of surfaces after polishing (**Fig. 3A**) and grinding (**Fig. 3B**). The surface expansion during grinding is much more significant, and the Sq coefficient is ten times higher, with the Sa of a similar value. As can be seen, the actual difference in peak heights for the

Table 3. Results of measurements of the surface topography of the tested samples. The black arrows indicate the directions of the counter-sample movement during tribological tests, white arrow indicate surface topography measurements direction

Tabela 3. Wyniki pomiarów topografii powierzchni badanych próbek. Czarne strzałki wskazują kierunki ruchu przeciwpółki podczas testów tribologicznych, a biała kierunek pomiaru topografii powierzchni

Machining type	Roughness (Gaussian filter, 250 μm)	Parameters, μm				
		Sq	Sa	Sp	Sv	Sz
Finishing milling		0.48	0.37	3.68	1.56	5.23
Spiral milling		0.51	0.43	3.34	2.60	5.94
Rough milling		0.79	0.46	5.37	20.30	25.67
Sanding		2.36	0.42	14.13	11.67	25.80
Polishing		0.15	0.47	3.14	2.35	5.50
Coarse flat grinding		1.53	0.50	8.34	6.22	14.53

Flat finishing grinding		0.36	0.57	2.16	1.91	4.06
Face grinding		0.16	1.05	4.55	1.50	6.05
Finishing turning		0.27	1.35	1.61	1.17	2.78
Rough turning		0.33	1.84	1.84	2.06	3.90

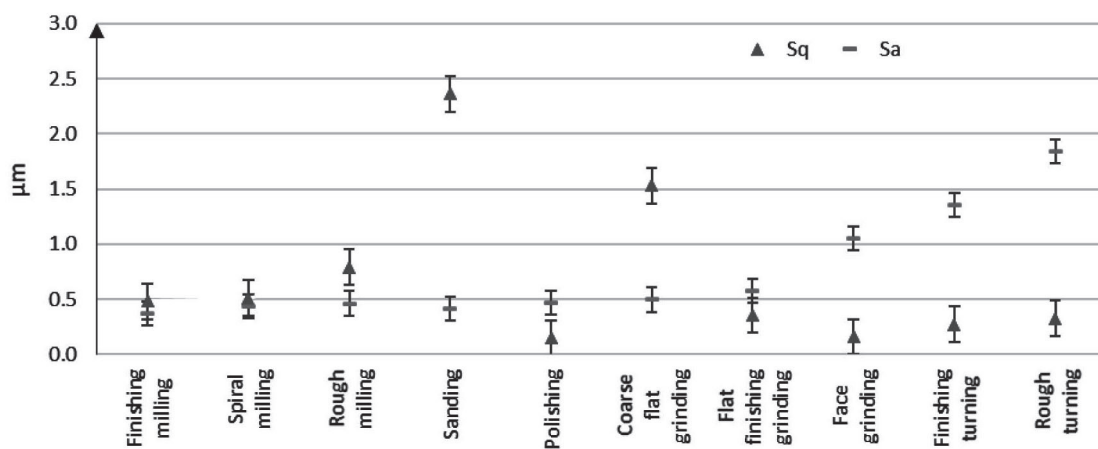


Fig. 2. The results of mean square deviation of the surface unevenness height from the reference plane Sq for each machining method and the arithmetic mean height of the surface Sa

Rys. 2. Wyniki średniego kwadratowego odchylenia wysokości nierówności powierzchni od płaszczyzny odniesienia Sq dla każdej metody obróbki oraz średniej arytmetycznej wysokości powierzchni Sa

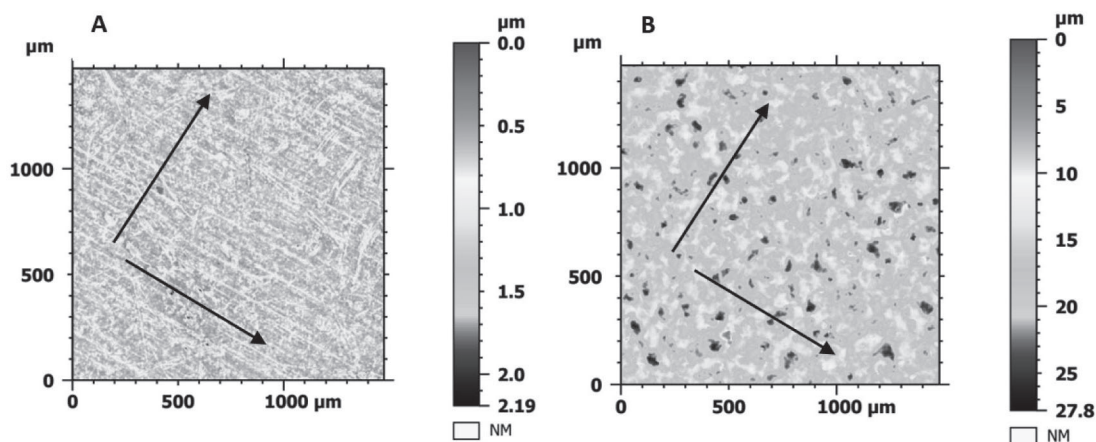


Fig. 3. Surface topography roughness after filtering with a Gaussian filter: A) polished sample, B) sanded sample. The arrows indicate the directions of the counter-sample movement during tribological tests

Rys. 3. Chropowatość topografii powierzchni po przefiltrowaniu filtrem Gaussa: A) próbki polerowanej, B) próbki szlifowanej. Strzałki wskazują kierunki ruchu przeciwpółki podczas testów tribologicznych

polished surface is about $0.5 \mu\text{m}$, and for the sanded sample, about $17.8 \mu\text{m}$. According to research by Zhou et al. [L. 15], the friction coefficient does not change unequivocally depending on the roughness of two bodies contact. For low frequencies of movement in the range of 2 Hz, the coefficient decreases with a decrease in roughness. The coefficient initially decreases and then increases for 4 Hz and 6 Hz values. This behaviour may indicate an optimal surface roughness area leading to a reduction in friction. The studies of Menezes et al. [L. 16] showed that the contact of the surface with higher roughness was characterised by a lower coefficient of friction for various materials, i.e. aluminium, steel, and copper. The author concludes that this decrease is due to the decreasing total contact area depending on the machining method.

The theoretical point of contact decreases with increasing roughness, which lowers the coefficient of friction. Sahin et al. [L. 17] noted lower friction coefficients for the contact of surfaces with higher roughness due to the decreasing total contact area. The author points out that this is mainly due to the surface treatment method. At the same time, however, the surface is damaged each time the tool passes, which boils down to "machining" it and generating a new topography with a roughness defined by the tool, the bearing ball. These transitions cause an abrasion of the ball and the sample surface (see Figs. 4B, 4D). It is noticeable that the transverse movement due to the unevenness resulting from the interaction of the tool with the treated surface deforms the base surface (see Fig. 4B). The cross-profile curve

confirms (see Fig. 4D) the observed effect. There is also some build-up of extra material along the sides of the path. In the case of movement parallel to the tool feed, the deformation is not noticeable. After careful analysis of the data is, a visible trace of the indenter obtained (see Fig. 4E). Therefore, it should be emphasised that the orientation of the indenter motion concerning the direction of topographic structures is essential for tribological problems. The transverse exposure (see Fig. 4B) causes the indenter ball to wear, while the parallel orientation (see Fig. 4A) reduces the ball to sliding along successive vertices. The width of the cavity bottom (see Fig. 4D) is approximately $120 \mu\text{m}$, which is close to the theoretical contact point diameter $d = 136 \mu\text{m}$. In the case of parallel movement, the value of the theoretical contact diameter suggests direct contact of the counter-sample with the surface at up to two points during the move.

Chips and built-up edges were observed in both motion cases. As indicated in Fig. 5, the materials left over from the friction process accumulate in the recesses of the surface topography (yellow colour). It should be noted that there is no apparent damage to the primary surface topography. The counter-test piece rubs on the surface of the protrusions (blue), leaving fragments of micro-chippings and oxides collected from the sample's surface in the recesses (yellow).

The result of the processes shown in Fig. 5 is that the system is partially "self-lubricated" to compensate for roughness peaks. On the one hand, the system automatically lubricates, allowing the oxide particles or fragments of samples to form

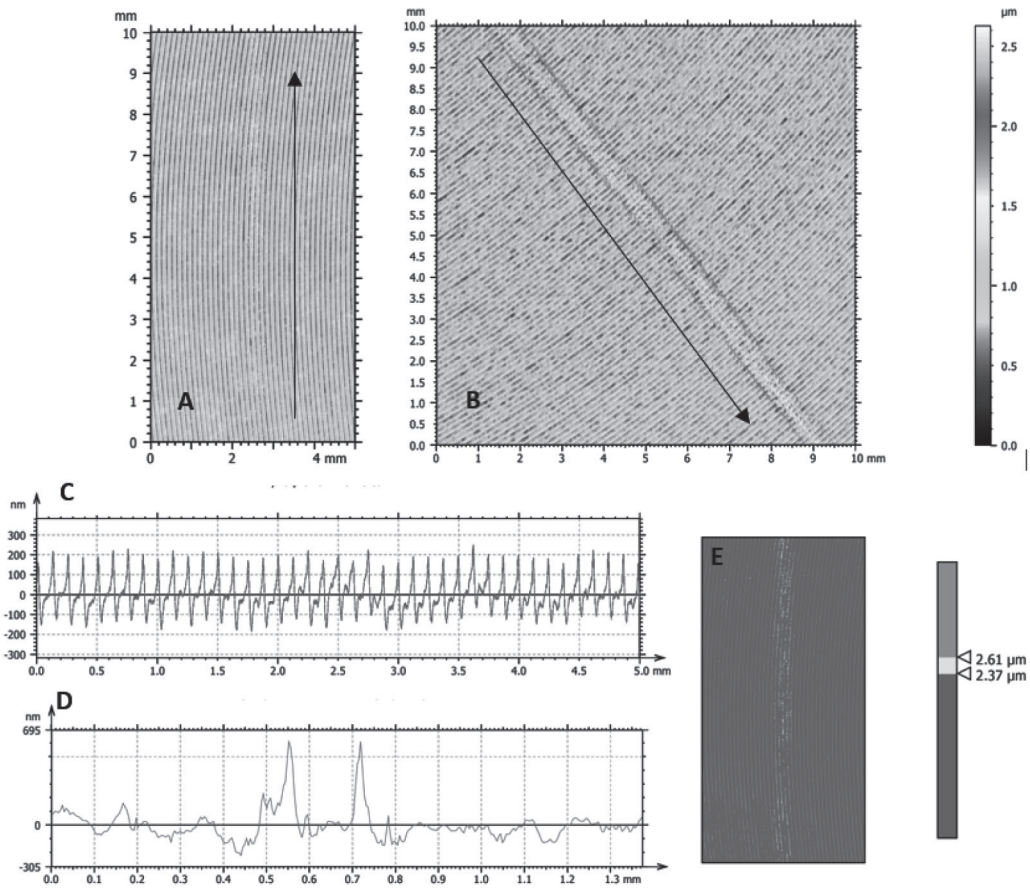


Fig. 4. Structure of the surface topography: A) for the movement parallel to the cutter path, B) for the movement perpendicular to the cutter path, as well as the mean profile curve for the path: C) parallel to the tool movement and D) perpendicular, E) indenter trace for the parallel movement after abstracting the data

Rys. 4. Struktura topografii powierzchni: A) dla ruchu równoległego do ścieżki freza, B) dla ruchu prostopadłego do ścieżki freza, a także krzywa profilu średniego dla ścieżki: C) równoległej do ruchu narzędzia oraz D) prostopadłej, E) ślad wglębnika dla ruchu równoległego po wyabstrahowaniu danych

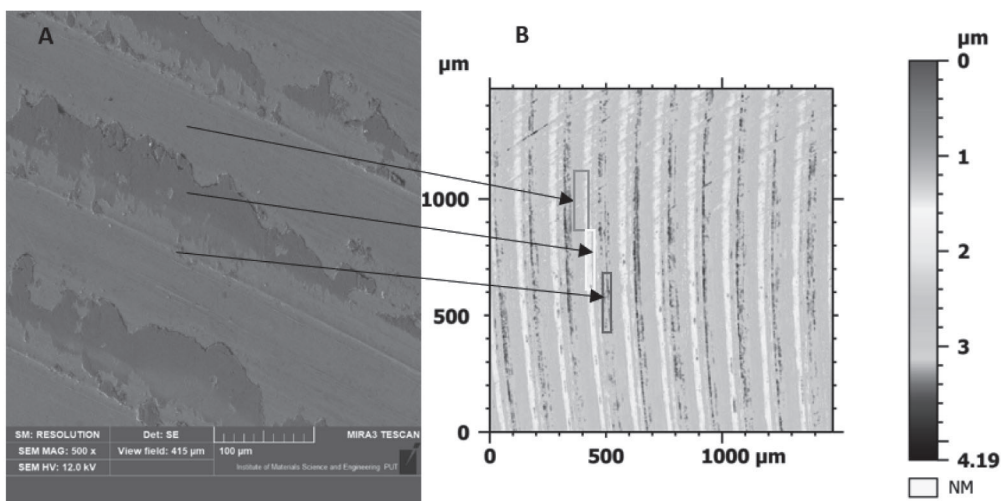


Fig. 5. SEM photo of the sample after tribological tests (A), 500x magnification, visibility of the surface build-up located in cavities, B) surface topography before the test

Rys. 5. Zdjęcie SEM próbki po badaniach tribologicznych (A), powiększenie 500x z widocznymi narostami powierzchni zlokalizowanymi w zagłębieniach, B) topografia powierzchni przed badaniem

a thin lubricating film. On the other hand, filling the space between the roughness peaks changes the surface topography, changing the contact surface

of the two surfaces. The analysis of the chemical composition of the accretions and confronting the results with the original properties of the sample are presented in **Tab. 4**.

Table 4. EDS measurement results – elemental composition of growths and surface of the sample subjected to turning and sandblasting after completed tribological tests

Tabela 4. Wyniki pomiarów EDS – skład pierwiastkowy narostów oraz powierzchni próbki poddanej obróbce toczeniem i piaskowaniu po przeprowadzonych testach tribologicznych

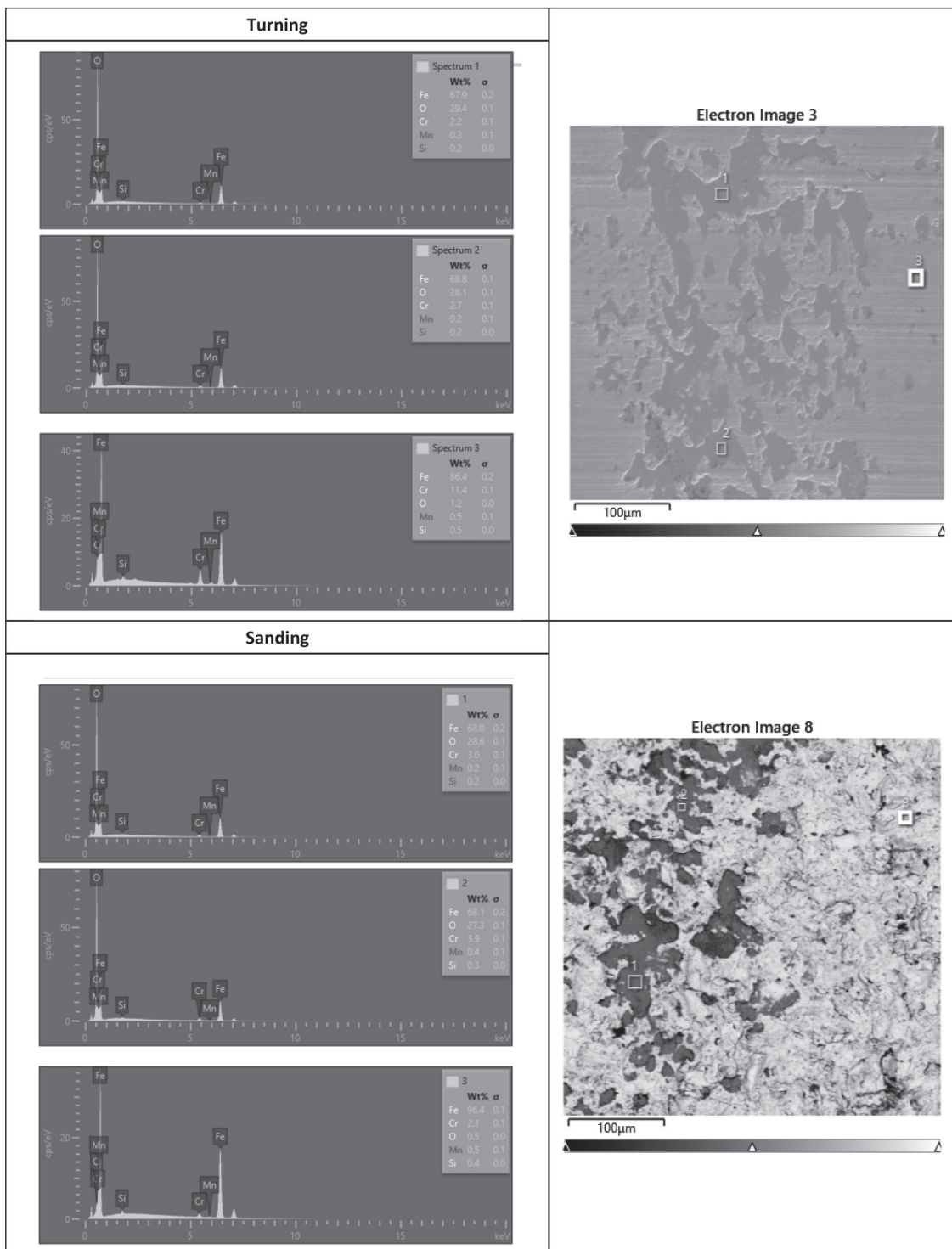


Table 4 presents a summary of the EDS measurements. In the case of both sandblasting and turning, the elemental composition data were collected at the indicated points. In both cases, in the traces following the passage of the bearing ball (Points 1 and 2), a decreased concentration of Fe was recorded, with a significant increase in the presence of O and Cr compared to the composition of the original sample surface. The results indicate the accumulation of oxides on the surface in the area of accretions caused by the interaction of the counter-sample with the sample surface. All samples were analysed. The results were consistent. Accumulation of oxides in the indicated space may result from both corrosions during the tribological process and their removal from the surface of the sample and application to the cavities of the surface. Aizawa et al. [L. 18] indicate that the presence of oxides

on the surface and oxides on the friction surfaces results in a tribofilm, a slip buffer. As shown in the research assumptions, the increased presence of oxides may reduce the friction coefficient. As can be seen in **Figures 4B** and **4D**, the presence of the oxides results in an increase in the contact surface of the counter-sample with the material by creating a specific "trough".

The results of the surface waviness measurements shown in **Fig. 6** were confronted with the theoretical size of the ball contact surface ($d = 136 \mu\text{m}$). The theoretical contact area is marked with a red dot in both graphs. A simulation of a ball-to-surface contact is shown in **Fig. 6C** and **Fig. 6D**. In **Fig. 6C**, a large number of peaks generate a large amount of waste filling the gaps (blue). The change in surface topography affects both the ball wear and the destruction of individual roughness peaks. This correlation is shown in **Tab. 5**.

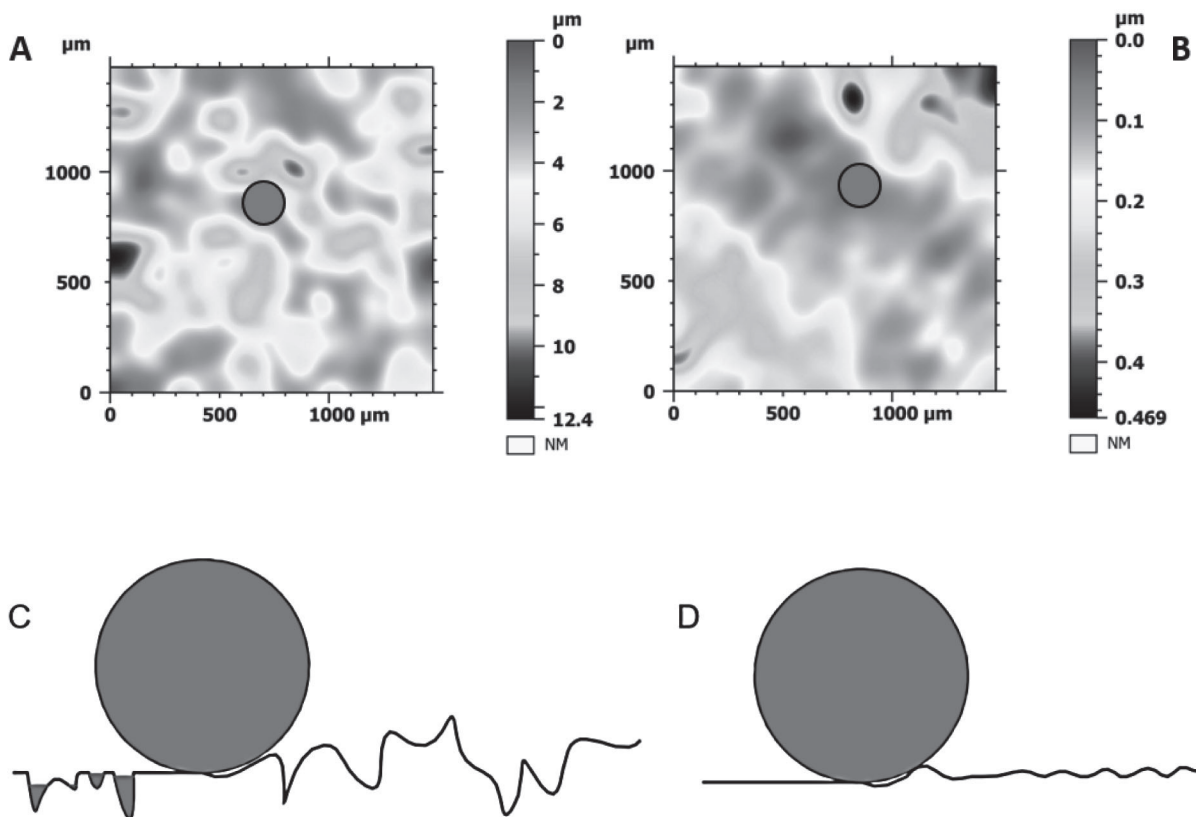


Fig. 6. Results of surface topography digitisation: A) waviness of the surface of a sanded sample, B) waviness of the surface of a polished sample, and an example of contact of a steel ball with the surface: C) surface after sanding, D) surface after polishing

Rys. 6. Wyniki digitalizacji topografii powierzchni: A) falistość powierzchni próbki szlifowanej, B) falistość powierzchni próbki polerowanej oraz przykład kontaktu kulki stalowej z powierzchnią: C) powierzchnia po szlifowaniu, D) powierzchnia po polerowaniu

Tribological tests

The tribological tests focused on assessing the behaviour of the friction coefficient in the initial stages of contact with the sample. Microscopic observations of the surface structure of the samples

showed that it had not been disturbed. Numerous adhesive deposits filling surface unevenness were noticed, which confirms the theory of smearing in the initial stages of the study. Photographs of the surface of the samples after testing are shown in **Figure 7**.

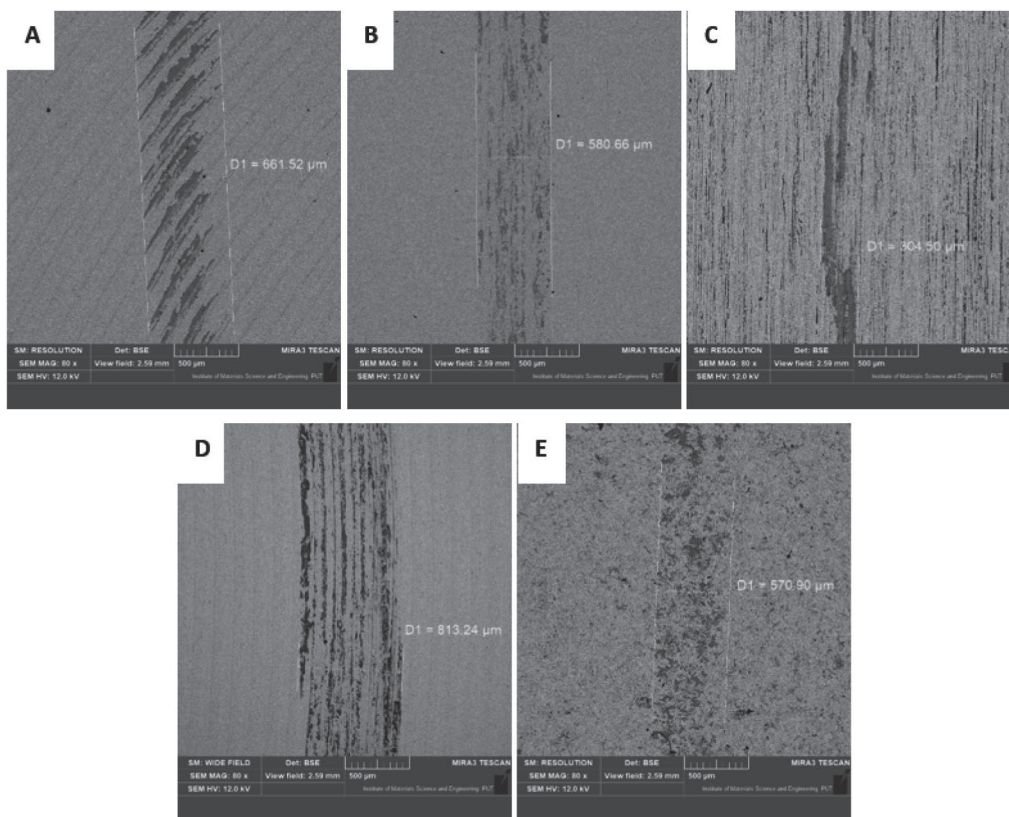


Fig. 7. Microscopic photos of the surface of the samples after the test: A) milling, B) polishing, C) grinding, D) turning, E) sanding

Rys. 7. Zdjęcia mikroskopowe powierzchni próbek po badaniu: A) frezowanie, B) polerowanie, C) szlifowanie, D) toczenie, E) szlifowanie

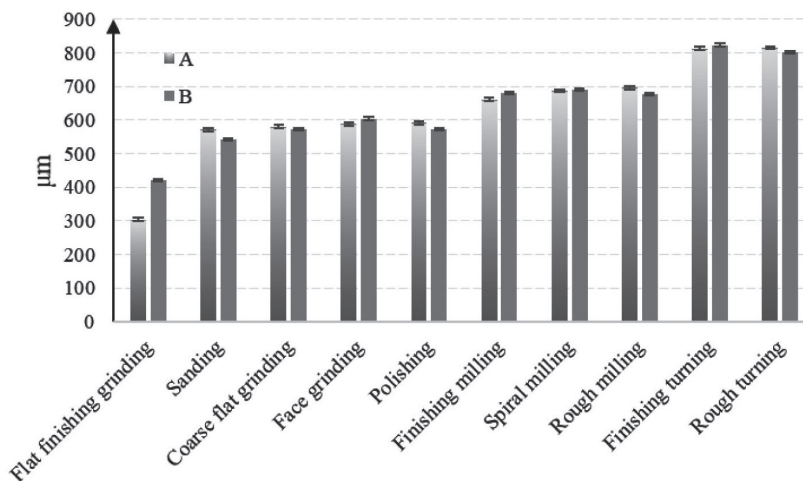


Fig. 8. Average wear path width obtained for individual machining methods and counter sample movement directions (A and B)

Rys. 8. Średnia szerokość ścieżki zużycia uzyskana dla poszczególnych metod obróbki i kierunków ruchu przeciwpółki (A i B)

The SEM images analysis (see **Fig. 7**) shows that the sphere's largest contact surface with the surface occurred in the case of surfaces after turning and milling, and the smallest in the case of flat finishing grinding (for both directions). The results of the track width measurements are also presented in **Fig. 7**. The SEM photos in all cases indicate the accumulation of abrasion products in the spaces of the sample surface topography.

The resulting paths are mainly growths. Slight differences in widths may indicate similar processes in the contact zone, despite the diversity of the surface topography. Using ImageJ, the surface area of the accretions was determined based on SEM photography. These analyses showed a clear relationship between the Sq coefficient and the surface area of the accumulations. The results are presented in **Table 5**. A decrease in the Sq value increases the size of the accretions.

Table 5. Comparison of the area covered by accretions in the SEM photo with the values of Sq and Sa parameters

Tabela 5. Porównanie powierzchni pokrytej przez narosty na fotografii SEM z wartościami parametrów Sq i Sa

Machining method	Area mm ²	Sq	Sa
Sanding	0.22	2.36	0.41
Grinding	0.27	0.68	0.71
Milling	0.32	0.60	0.42
Turning	0.33	0.30	1.59
Polishing	0.34	0.15	0.46

An important feature noticed during the tests is the character of the course of the friction coefficient during the measurement. The courses of the friction coefficient do not differ from each other, depending on the orientation, concerning the topographic structure of the surface for individual methods. The directions of measurements are indicated in

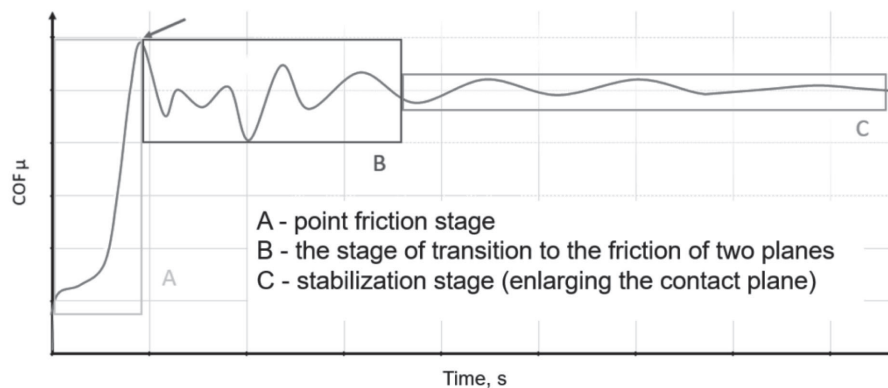


Fig. 9. Diagram of the course of changes in the coefficient of friction in time

Rys. 9. Wykres przebiegu zmian współczynnika tarcia w czasie

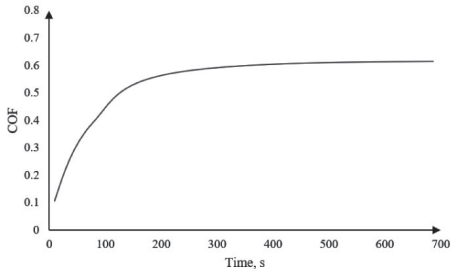
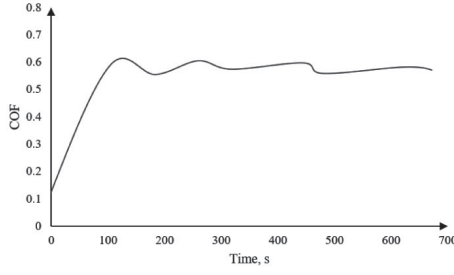
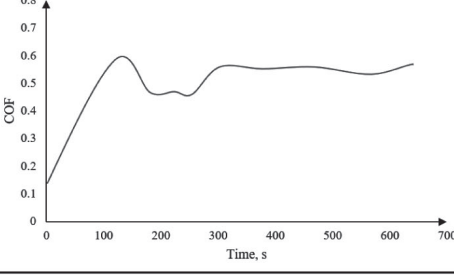
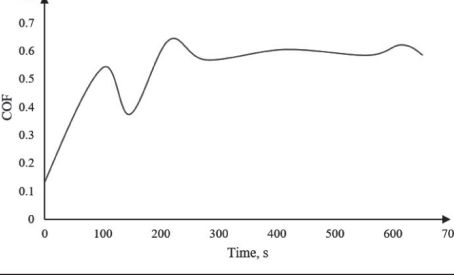
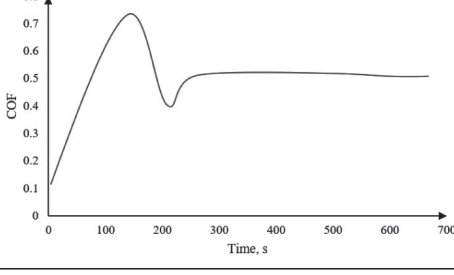
Tab. 6. It was confirmed that the coefficient of friction at the beginning and end of the runs are similar for all analysed cases. The starting threshold was in the range of 0.1–0.2, and the ending was in the field of 0.4–0.6. These values have been confirmed. Significant differences were noticed between the points mentioned above, i.e. three stages of the course of the friction coefficient as a function of time were distinguished (see **Fig. 9**).

The point friction stage (see **Fig. 9**) is the shortest in the course of changes in the coefficient of friction with time. There is a point or multi-point contact of the sphere with the surface. The sphere touches at the highest peaks of the roughness. This stage turns into a transition to the friction of two

planes; the course of which can be described as chaotic and difficult to define unequivocally. In step B, new surface topography is constituted by destroying the roughness peaks. Fluctuations in the friction force, and thus in the friction coefficient, are caused by the irregularity of the surface. The ball simultaneously destroys the topography and fills the cavities in the topography with cutting products. The ball itself is also subject to abrasive wear. The formation of new surface topography is noticeable in stage C, stabilising the friction coefficient. Similar research results were obtained by Boneh et al. [**L. 19**], showing the three stages of stabilisation of the friction coefficient. The research showed the following stages: wear by the failure of

Table 6. Summary of the maximum mean square deviation of the surface Sq and the course of the friction coefficient in time

Tabela 6. Zestawienie maksymalnego odchylenia średniokwadratowego powierzchni Sq i przebiegu współczynnika tarcia w czasie

Method	Sq_{max}	COF
Sanding	2.65 ± 0.1	
Grinding	1.65 ± 0.1	
Milling	0.60 ± 0.08	
Turning	0.34 ± 0.06	
Polishing	0.16 ± 0.02	

isolated asperities associated with roughening of the fault surface, the subsequent failure of many asperities, the reduction of the friction coefficient, and finally, the steady-state stage.

The research showed an interesting relationship between the values of the maximum mean square deviation of the surface unevenness height from the reference plane Sq_{max} . The higher the value of Sq_{max} ,

the less chaotic the course of changes in the friction coefficient is, gradually increasing (see **Tab. 6**). In the case of sanding ($Sq_{max} = 2.65 \pm 0.1$), the course of the friction coefficient is regular, a stable point friction stage is noticeable, and then the transition to the coefficient stabilisation, without a marked transition to the friction of two planes. Therefore, it can be concluded that point friction and planes with a fast stabilisation time are noticeable in this case. In the case of grinding ($Sq_{max} = 1.65 \pm 0.1$), the point friction stage is short and increases quickly, and then the friction of the plane occurs without the chaotic stage distinguished. All three steps are noticeable in the case of milling ($Sq_{max} = 0.61 \pm 0.08$) and turning ($Sq_{max} = 0.34 \pm 0.06$). Still, for milling, the value of the friction coefficient for the moment of transition from the point friction phase to the stage of transition to the friction of two planes is equal to the coefficient for stabilised friction. In the case of turning, this value is significantly lower. During the polished surface examination ($Sq_{max} = 0.16 \pm 0.02$), the friction coefficient reaches its maximum at the moment of transition from the point friction stage to the friction of two planes and is higher than the stable value. Therefore, the larger the active surface, the more stable the process of achieving the target value of the friction coefficient.

During the research, the duration of individual stages of shaping the coefficient of friction was

also determined. The average time of stabilisation of the coefficient of friction – i.e. going through steps A and B – was $t_{avg} = 222$ s. It was similar for all cases. At this level, no differences between the surface shaping methods were noticed. The values of the coefficient of friction after stabilisation are convergent in all cases and do not differ significantly from each other. The measurement results are presented in **Fig. 10** (for both directions A and B)

As indicated in the graphics in **Tab. 6** and **Fig. 3**, the measurements of the friction coefficient took place in two directions. The directionality of the counter-sample's movement in relation to the surface geometry structure did not show any unequivocal effect on the value of the friction coefficient. In order to show a clear dependence, a larger number of tests should be carried out, aimed at showing these dependence.

Additionally, measurements were also carried out to analyse the results obtained in **Tab. 4**. The ball moved in a circle (running along the same path) and in a spiral (each time rubbing against a new surface). The test was carried out on the surface of a sanded sample. In the case of circular motion, the result was similar to the previous tests, and significant differences were noticed in the case of the spiral motion test. The list of both cases is presented in **Figure 8**. The purpose

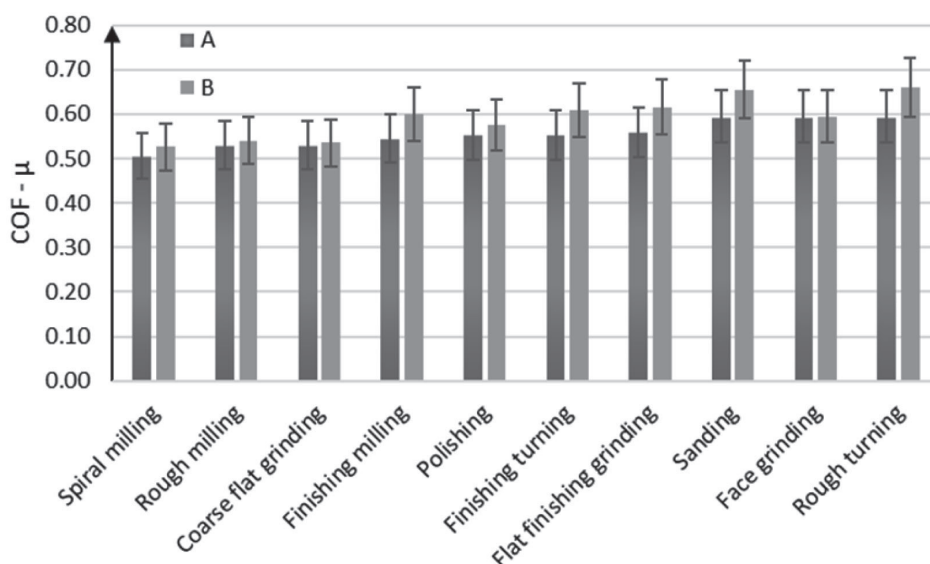


Fig. 10. Coefficient of friction after stabilisation (stage C) for all analysed surfaces, for directions A and B marked in the **Tab. 6**

Rys. 10. Współczynnik tarcia po stabilizacji (etap C) dla wszystkich analizowanych powierzchni, dla kierunków A i wskazanych w tabeli 6

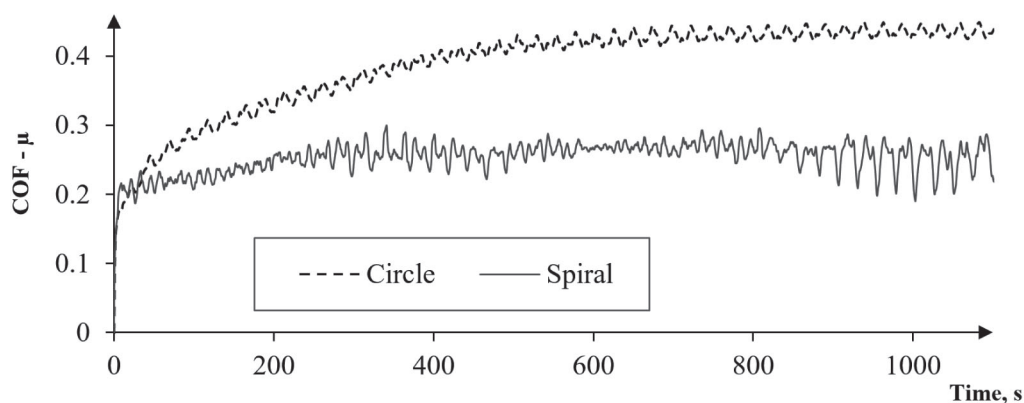


Fig. 11. Time-dependent value of the coefficient of friction for circular and spiral motion on the surface of the sample after sandblasting

Rys. 11. Wartość współczynnika tarcia zależna od czasu dla ruchu kołowego i spiralnego na powierzchni próbki po piaskowaniu

of the measurement was to show that moving along a new path causes encountering undamaged roughness peaks that lower the coefficient of friction. Additionally, in the case of a constant track, a higher value of the friction coefficient is obtained with greater stability of the measurement. The possible influence of oxides as self-lubricating elements of the system was also assumed.

The test results indicate the possibility of a significant influence of the presence of oxides accumulated in the surface layer on the friction coefficient. Following the results obtained by Merz et al. [L. 20] during the tests, an oxide layer at the micron or even nanometre level is constantly recreated on the surface in cyclic abrasive contact. It directly influences the course of abrasive wear. Cho et al. [L. 21] indicated similar properties, noting that the larger the oxide layer, the wider is the low friction region. As Hager et al. [L. 22], the contact of highly oxidised steel surfaces gives a friction coefficient similar or lower than that of untreated steel surfaces lubricated with oil in rolling/sliding friction. Similar results were obtained in the above study. It can be assumed that, in the initial stages of contact, the oxides act as a lubricant, lowering the value of the frictional force (see Fig. 11), stabilising the wear process in the further stages of contact. Tearing material off the peaks of the roughness and transporting them into the depressions changes the topography of the path. It is related to the increase of the surface contact zone (an increase of the friction coefficient and its stabilisation). Interestingly, the clear difference in the values of the friction coefficient for circular

and spiral motion suggests that motion along the contact surface with roughness peaks may be a positive phenomenon. This is due to the reduced contact area (longer stay in the point contact zone). It can significantly extend the life of the friction pair elements, although it is characterised by low stability.

CONCLUSIONS

The study concerning the evaluation of the tribological properties of hardened surfaces constituted by various methods of machining allowed us to draw the following conclusions:

1. There are noticeable differences in the friction coefficient values as a function of the path for samples produced with different machining methods.
2. The initial and final values of the friction coefficient for the different methods are similar.
3. An increase in the value of the maximum root mean square deviation of the surface roughness from the reference plane Sq_{max} for dry tests does not increase the value of the friction coefficient, but it does correlate with the amount of built-up edges during machining.
4. The surface topography resulting from a specific machining method affects the course of COF changes, but there is no clear effect of the directionality of the geometric structure on COF.
5. The transition time to total two-plane friction (Stage A and B) is similar for all methods.

6. The more significant the active surface (sanding), the more stable the process of reaching the target COF is – the contact area increases.
7. The oxides in the top layer potentially stabilise the coefficient of friction.

REFERENCES

1. Nosal S.: Tribology. Introduction to the issues of friction, wear and lubrication. Poznan, 2012.
2. Dmochowski J.: The basics of machining. 3 red. Warszawa, 1983.
3. Feld, M., Machine building technology. 3 red. Warszawa, 2000.
4. Attabi, S., Himour, A., Laouar, L., Motallebzadeh, A. Effect of Ball Burnishing on Surface Roughness and Wear of AISI 316L SS. *Journal of Bio- and Tribo-Corrosion*. 7, 2021.
5. Grzesik W.: The influence of surface topography on the operational properties of machine parts. *Mechanik*, 8–9, 2015, pp. 587–593.
6. Sedlacek M., Podgornik B. Vizintin J.: Influence of surface preparation on roughness parameters, friction and wear. *Wear*, 7, 2008, pp. 482–487.
7. Garcia-Leon R., Martinez-Trinidad J., Campos-Silva I., Figureos-Lopez U., Guevara-Morales A.: Wear maps of borided AISI 316L steel under ball-on-flat dry sliding conditions. *Materials Letters*, 282, 2021, pp. 128842.
8. Linhu T., Chengxiu G., Huang J., Zhang H., Chang W.: Dry sliding friction and wear behaviour of hardened AISI D2 tool steel with different hardness levels. *Tribology International*, 66, 2021, pp. 165–173.
9. Riadh A., Mounir K., Fakhreddine D.: Friction and Wear Behavior of Steels under Different Reciprocating Sliding Conditions. *Tribology Transactions*, 55, 2012, pp. 590–598.
10. Feld, M. Basics of designing technological processes of typical machine parts. Warszawa, 2000.
11. Correia J.A.F.O., Jesus de A.M.P., Fernandes A.A., Calçada R.: *Mechanical Fatigue of Metals. Experimental and Simulation Perspectives*. Springer, 2019.
12. SAE Ferrous Materials Standards Manual, HS-30, Society of Automotive Engineers, 1999.
13. Davis J.R.: *ASM Specialty Handbook – Carbon and Alloy Steels*, ASM International, Metals Park, 1996.
14. Chung-Woo C., Young-Ze L.: Effects of oxide layer on the friction characteristics between TiN coated ball and steel disk in dry sliding. *Wear*, 297, 2003, pp. 383–390.
15. Zhou Y., Zhu H., Zhang W., Zuo X., Li Y., Yang J.: Influence of surface roughness on the friction property of textured surface. *Advances in Mechanical Engineering*, 7, 2015, pp. 722–730.
16. Menezes P.L., Kishore Kailas S.V.: Influence of roughness parameters on coefficient of friction under lubricated conditions. *Sadhana*, 33, 2008, pp. 181–190.
17. Sahin M., Çetinarslan C.S., Akata, H.E.: Effect of surface roughness on friction coefficients during upsetting processes for different materials. *Materials & Design*, 28, 2007, pp. 633–640.
18. Aizawa T., Mitsuo A., Yamamoto S., Sumitomo T., Muraishi S.: Self-lubrication mechanism via the in situ formed lubricious oxide tribofilm. *Wear*, 259, 2005, pp. 708–718.
19. Boneh Y., Chang J.C., Lockner D.A., Reches Z.: Evolution of Wear and Friction Along Experimental Faults. *Pure and Applied Geophysics*, 171, 2014, pp. 3125–3141.
20. Merz R., Brodyanski A., Kopnarski M.: On the Role of Oxidation in Tribological Contacts under Environmental Conditions. *Conference Papers in Science*, 2015, pp. 1–11.
21. Cho C.-W., Lee Y.-Z.: Effects of oxide layer on the friction characteristics between TiN coated ball and steel disk in dry sliding. *Wear*, 254, 2013, pp. 383–390.
22. Hager C.H., Evans R.D.: Friction and wear properties of black oxide surfaces in rolling/sliding contacts. *Wear*, 338–339, 2015, pp. 221–231.